



● *Original Contribution*

IN VIVO TIME HARMONIC ELASTOGRAPHY OF THE HUMAN HEART

HEIKO TZSCHÄTZSCH,* THOMAS ELGETI,* KATRIN RETTIG,* CHRISTIAN KARGEL,[†] ROBERT KLAUA,[‡]
 MICHAEL SCHULTZ,[‡] JÜRGEN BRAUN,[§] and INGOLF SACK*

*Department of Radiology; Charité–Universitätsmedizin Berlin, Campus Charité Mitte, Berlin, Germany; [†]Institute for Measurement and Automation, Division of Sensor Technology and Measurement Systems, Bundeswehr University Munich, Neubiberg, Germany; [‡]G.A.M.P.T.mbH, Merseburg, Germany; and [§]Institute of Medical Informatics; Charité–Universitätsmedizin Berlin, Campus Benjamin Franklin, Berlin, Germany

(Received 21 June 2011; revised 4 November 2011; in final form 5 November 2011)

Abstract—Time harmonic elastography is introduced as a modality for assessing myocardial elasticity changes during the cardiac cycle. It is based on external stimulation and real-time analysis of 30-Hz harmonic shear waves in axial direction of a parasternal line of sight through the lateral heart wall. In 20 healthy volunteers, the externally induced waves showed smaller amplitudes during systole ($76.0 \pm 30.8 \mu\text{m}$) and higher amplitudes during diastole ($126.7 \pm 52.1 \mu\text{m}$). This periodic wave amplitude alteration preceded ventricular contraction and dilation by about 100 ms. The amplitude ratio of 1.75 ± 0.49 indicates a relative change in myocardial shear elasticity on the order of 14 ± 11 . These results well agree with observations made by cardiac magnetic resonance elastography for a similar displacement component and region of the heart. The proposed method provides reproducible elastodynamic information on the heart in real-time and may help in diagnosing myocardial relaxation abnormalities in the future. (E-mail: ingolf.sack@charite.de) © 2011 World Federation for Ultrasound in Medicine & Biology.

Key Words: Myocardial shear modulus, Continuous harmonic waves, Shear wave energy flux, Ultrasound elastography, MR elastography, Isovolumetric times, Cardiac contraction, Cardiac relaxation, Real-time strain estimation.

INTRODUCTION

The heart's capability to circulate blood through the cardiovascular system is directly related to the periodic alteration of myocardial elasticity. Contraction and relaxation of the heart is primarily effected by the alteration of the myocardial shear modulus, which thus represents the physical quantity behind pressure generation inside the ventricle. Direct measurement of the myocardial shear modulus may, thus, help in assessing myocardial dysfunction and relaxation abnormalities (Zile et al. 2004; Aurigemma et al. 2006).

Elastography enables the noninvasive measurement of mechanical parameters of *in vivo* soft tissue (Ophir et al. 1991) with emerging clinical applications from breast tissue characterization to cardiology (see [Wells and Liang 2011] and references therein). There are several

approaches to elastography of the heart and the cardiovascular system. Various researchers exploited intrinsic activation of myocardium (Konofagou et al. 2002; Varghese et al. 2003; Kanai, 2005; Lee et al. 2011) or arteries (Maurice et al. 2008; Schaar et al. 2005; Vappou et al. 2010). Other approaches rely on extrinsic activation by modulating the ultrasonic radiation force (Hsu et al. 2007; Bouchard et al. 2009; Pislaru et al. 2009; Nenadic et al. 2011; Dumont et al. 2011) or sending time harmonic shear waves through the chest (Elgeti et al. 2008; Sack et al. 2009). The resulting strain fields can be determined using ultrasound (Ophir et al. 1991; Parker et al. 1990) or magnetic resonance imaging (MRI) (Plewes et al. 1995; Muthupillai and Ehman, 1996). While medical ultrasound is rather inexpensive, robust and capable of strain estimation in real-time, phase-contrast MRI has the advantage of being intrinsically sensitive to motion in three dimensions, which is particularly useful for elastography. However, cardiac MR elastography (MRE) suffers from long scanning times since images are reconstructed from lines acquired in synchrony with the electrocardiogram (ECG) over multiple heart beats (Rump et al. 2007; Sack et al. 2009;

Address correspondence to: Ingolf Sack, Ph.D., Department of Radiology, Charité–Universitätsmedizin Berlin, Charitéplatz 1, 10117 Berlin, Germany. E-mail: ingolf.sack@charite.de

Disclosure of a potential conflict of interest: R.K. and M.S. are employees of G.A.M.P.T.mbH, Merseburg, Germany.

Robert et al. 2009; Kolipaka et al. 2010). This periodicity of signal acquisition requires a periodic mechanical stimulus matched with the repetition time of the MRI sequence. For this reason, the time harmonic wave approach is most appealing in cardiac MRE since the synchronization of image acquisition and periodic mechanical stimulation causes steady states in both MR signal dynamics and mechanical tissue response (Bieri et al. 2006; Rump et al. 2007). The mechanical steady state sustains a constant flux of wave energy through the heart, which is a prerequisite for analyzing the variation of shear wave amplitudes over the cardiac cycle.

It must be pointed out that the actuation plate in MRE vibrates in the direction of the anterior-posterior axis of the patient inducing primarily compression waves into the chest. However, these compression waves are scattered at tissue boundaries yielding shear waves, which provide the desired source of elasticity contrast between the contracted and the relaxed state of the myocardium. Cardiac shear waves were identified in MRE essentially by their dynamics over the heart cycle. It was demonstrated that wave amplitudes decrease in early systole, *i.e.*, synchronously with the rise of ventricular pressure (Elgeti et al. 2009). Contrary, in early diastole, wave amplitudes increase when ventricular pressure decreases. It is most notable that this alteration of wave amplitudes during the cardiac cycle precedes the change in ventricular volume similarly to the ventricular pressure change, which defines the well-known isovolumetric cardiac phases (Elgeti et al. 2010b). This wave amplitude variation effect, the so-called WAV effect (Sack et al. 2009), was demonstrated by MRE mainly for two components of the wave field: the in-plane component along anterior-posterior direction and the through-plane component as illustrated in Figure 1. We here apply the principle of WAV-MRE to ultrasound elastography. Our hypothesis is twofold: (1) continuous harmonic vibrations of the heart of similar frequency as used in WAV-MRE can be delineated in real-time using a dedicated A-scan ultrasound device; and (2) the WAV effect can be measured by considering only one displacement component along the axial ultrasound beam direction corresponding to the through-plane displacement component in MRE. These hypotheses are tested in 20 healthy volunteers. Similar to what has previously been reported for MRE (Sack et al. 2009), we will measure relative elasticity ratios derived from the ratio of wave amplitudes during diastole and systole. Furthermore, we estimate elasticity-based isovolumetric cardiac time intervals as reported in (Elgeti et al. 2010b). If successful, the proposed ultrasound method can provide similar information as accessible by cardiac MRE, however, in real-time and at a fraction of the costs of an MRI examination. Our intention was to transfer the knowledge gained by cardiac MRE about wave field polarization in the heart to an ultrasound

method capable of providing real-time feedback of shear wave amplitudes. Using such an ultrasound set-up, cardiologists may assess myocardial relaxation abnormalities by means of myocardial shear modulus variations in a time- and cost-efficient way.

METHODS

Subjects

The study was approved by the local ethics committee and the responsible authorities (DIMDI –Reg. No. DE/CA73/5967/10). Written informed consent was obtained from each volunteer prior to inclusion. The group size was estimated by a power analysis based on wave amplitude data measured by cardiac MRE in the septum of 18 healthy male volunteers. With mean values for systolic and diastolic wave amplitudes of 0.21 ± 0.06 mm and 0.31 ± 0.09 mm, respectively, a group size of 20 volunteers was predicted by assuming a power of 90%. None of the 20 volunteers (age: 30.5 ± 8.1 years, range: 25–40 years) was on any medication, nor had any history of cardiac events, hypertension, diabetes or hypercholesterolemia. The group-averaged weight was 81.8 ± 12.5 kg with an averaged body height of 181.8 ± 7.8 cm. Two volunteers were overweight presenting a body mass index (BMI) of 31.9 and 26, respectively. These two volunteers showed normal systolic and diastolic function in transthoracic echocardiography.

Ultrasound imaging and elastography

Volunteers were investigated in expiration in a left lateral recumbent position. Prior to elastography, all volunteers were scanned using standard B-mode ultrasound to locate the position of the left ventricular lateral wall (Fig. 2a). For elastography, a custom-designed pulse wave, A-mode ultrasound device equipped with a 2 MHz single-element transducer with a diameter of 16 mm and 70 mm focal depth (G.A.M.P.T.m.b.H., Merseburg, Germany) was dedicated to real-time signal processing by a 50-MHz integrated analog-digital converter connected to a standard 3-GHz dual core PC via 480 Mbit/s USB port. Ultrasound pulse repetition frequency (PRF) was 840 Hz, yielding 28 echo signal segments per vibration period of 30 Hz. The A-line acquisition window of ≈ 30.7 mm length (2^{11} samples) was positioned so that it started at approximately 60 mm depth, depending on the position of the myocardial wall. Within this window, a subwindow of ≈ 15.4 mm length (2^{10} samples) was manually selected for real-time signal processing. The memory sweep cycle for the display of displacement signals on the monitor was 7.1 s.

Mechanical stimulation of shear waves

The mechanical actuator was built from a loudspeaker connected to a vibration plate (size 10×30 cm²),

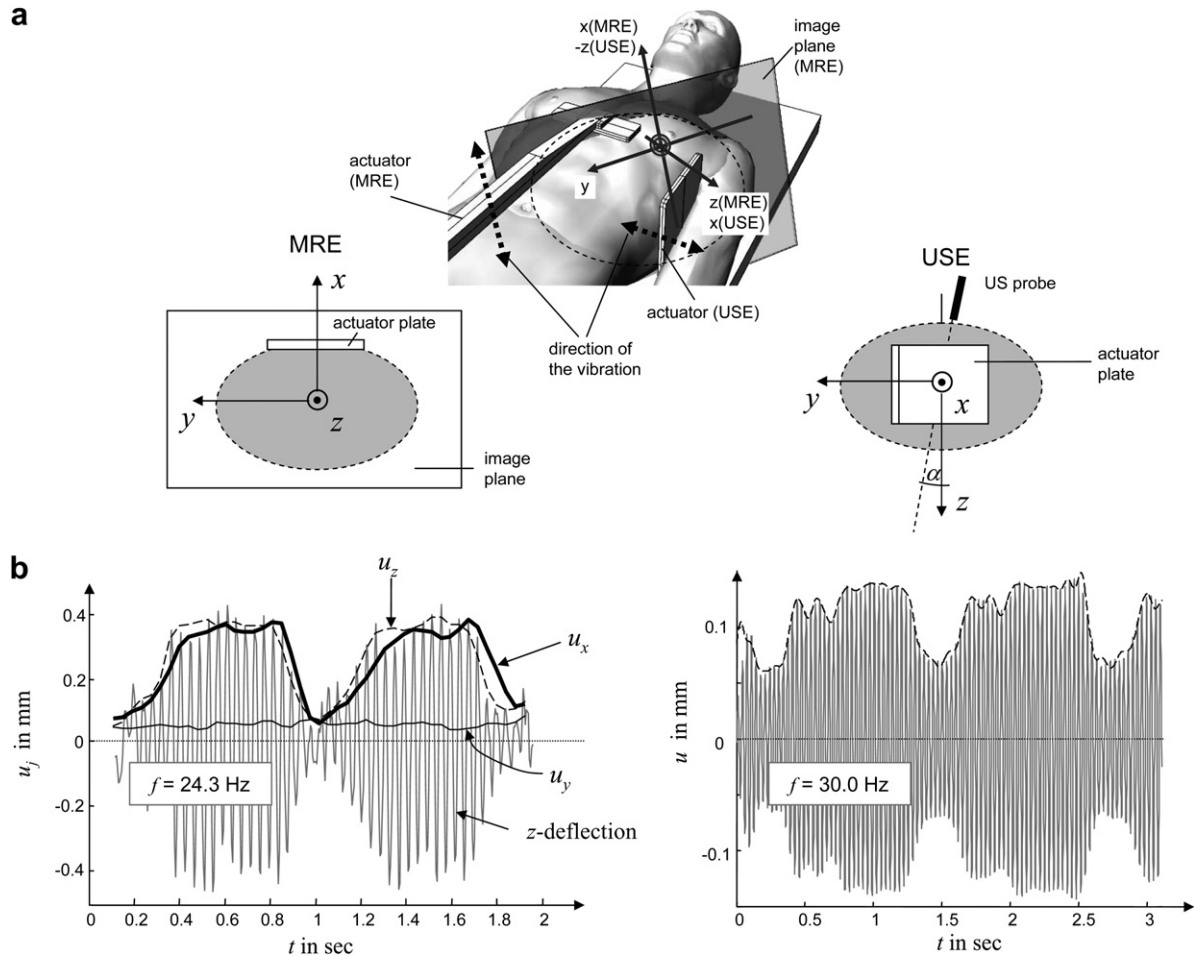


Fig. 1. The hypothesis in ultrasound-based time harmonic cardiac elastography (USE) was derived from observations made by magnetic resonance elastography (MRE). (a) Coordinate systems used in MRE and USE. Please note, in USE, the patient is not in supine position but in lateral recumbent position as indicated in Figure 2. Therefore, in USE, the waves are induced beneath the lateral side of the chest, which is approximately perpendicular to the actuator position in MRE. The axial motion component in USE along a parasternal line of sight is similar to the through-plane (u_z) component in MRE. (b) Left hand side: Wave amplitudes measured by MRE in all three Cartesian directions corresponding to the coordinates given in (a). The data are taken from (Sack *et al.* 2009). Typically, the u_y component shows no or only minor variation in amplitude over the cardiac cycle. Right hand side: Considering a small angle α , USE as shown in (a) allows us to mainly measure the u_z component along the axial direction of the ultrasound beam and, thus, to analyze a similar wave amplitude variation (WAV) effect as observable in MRE.

which was placed on the examination table underneath the volunteer's left lateral side of the chest (Fig. 2b). For the positioning of the actuator no individual variation of heart anatomy or body shape was taken into account. The loud-speaker was driven by a sinusoidal alternating current of 30 Hz by a function-generator-controlled audio amplifier. The steady-state vibration amplitude of the actuator was manually adjusted by the operator during the examination with approximately a few millimeters of surface deflection. To compare the results of this ultrasound-based investigation with those of cardiac MRE, a similar shear wave frequency as in MRE is required. We chose a frequency of 30 Hz to compromise between higher excitation

frequencies, which are well separated from intrinsic heart motion but cause various physical wave properties that at current are still unexplored due to the lack of *in vivo* cardiac MRE data, and lower frequencies of about 25 Hz as applied in MRE due to the smaller damping and the constant flux of wave energy through the heart. In three volunteers, the vibration level was changed in consecutive experiments from zero to the maximum vibration level within a range considered the comfort range, *i.e.*, no discomfort due to external mechanical stimulation was encountered. Two experiments were run in all volunteers: one without vibration and another with a medium vibration level defined from the averaged subjective sensations

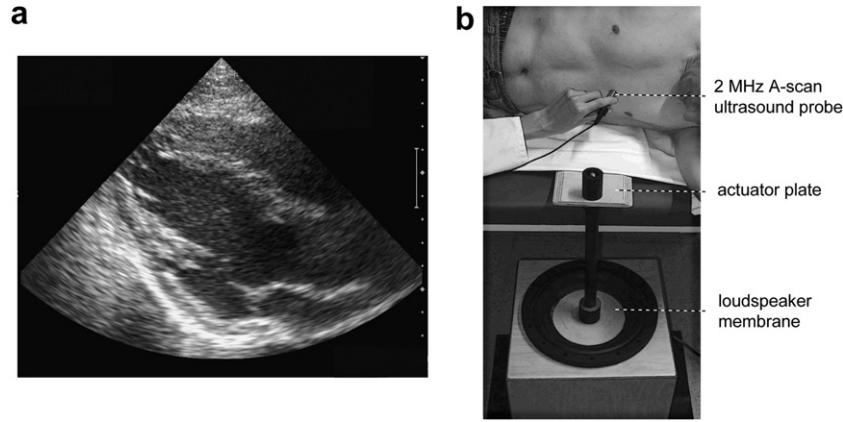


Fig. 2. Experimental set-up of time-harmonic cardiac elastography. (a) B-mode of the heart's long axis from a parasternal view as used for image guidance in A-line elastography. The target region for vibration measurements was in the inferior wall. (b) Continuous harmonic vibrations were induced from the lateral side of the chest by an actuator plate mounted to a loudspeaker.

reported by all volunteers. The entire examination time per volunteer including B-mode prescan and elastography was approximately 5 min.

Real-time signal processing

We assume that axial tissue displacement is a linear superposition of intrinsic motion of the heart wall (u_{card}) and three anharmonic oscillations with the first-harmonic frequency f :

$$U(t_k, x_l) = u_{card}(t_k, x_l) + \sum_{m=1}^3 u_m(t_k, x_l) \sin(2m\pi f t_k). \quad (1)$$

t_k and x_l are the discrete time and position, respectively, with increments corresponding to the "slow time" sampling by $\Delta t = 1/\text{PRF}$ (≈ 1.2 ms) and the "fast time" radio-frequency (RF) sampling of $\Delta x = 0.15$ mm. In eqn (1), higher harmonics of $m > 3$ are ignored as we consider their amplitudes to rapidly decline due to viscous damping and the widely harmonic vibration of the actuator at frequency f . Nevertheless, the terms of $m = 2$ and $m = 3$ are kept here as we will show later, how higher harmonics are eliminated from the principal vibration signal. According to Figure 1, U corresponds to the through-plane MRE component u_z provided that angle α is small.

A time-discrete estimate of the deflection velocity dU/dt was calculated by cross-correlating in-phase/quadrature-phase signals $\underline{I}(t_k, x_l)$ and $\underline{I}(t_{k-1}, x_l)$ derived from consecutively acquired RF A-line signals and searching for the zero-crossing of the phase (\angle) of the estimated complex cross-correlation function $\hat{R}(\Delta U)$:

$$\dot{U}(t_k - \Delta t/2) = \frac{1}{\Delta t} \min_{\Delta U} \left\{ \left| \angle \hat{R}(\Delta U) \right| \right\} \text{ with}$$

$$\hat{R}(\Delta U) = \sum_{l=1}^N \underline{I}(t_{k-1}, x_l + \Delta U) \cdot \underline{I}^*(t_k, x_l) \quad (2)$$

Underlined symbols represent complex signals, the asterisk indicates the complex conjugate and ΔU is the (continuous) displacement lag parameter. $N = 2^{10}$ denotes the size of the spatial processing subwindow. Since in our case cardiac motion is about two orders of magnitude larger than the applied extrinsic vibrations, u_{card} was approximated by the cumulative sum of $\dot{U}(t_k)$:

$$u(t_k)_{card} \approx U(t_k) = \Delta t \sum_{n=1}^k \dot{U}(t_n) + C. \quad (3)$$

C is an arbitrary integration constant that takes into account static offsets. $U(t_k)$ still comprises all motion components considered in eqn (1) averaged over the spatial processing window (≈ 15.4 mm size). Our goal was to separate the time-dependent amplitude variation u_1 of the first harmonic from higher harmonic vibrations, u_m , $m = 2, 3$ and from cardiac motion. A feasible time-efficient way for suppressing u_{card} was found by subtracting the temporal mean of \dot{U} within a moving average window of size $1/f$:

$$\dot{U}(t_k)_{highpass} = \dot{U}(t_k) - \frac{1}{f\Delta t} \sum_{n=k-\frac{1}{2f\Delta t}}^{k+\frac{1}{2f\Delta t}} \dot{U}(t_n). \quad (4)$$

In $\dot{U}_{highpass}$ cardiac tissue velocity u_{card} is efficiently suppressed if it is constant over a vibration period. This assumption was sufficiently well matched in our experiments. We proceed with considering higher harmonic motion components of the externally induced 30-Hz vibration. In good approximation, a band pass filter response centered at driving frequency can be achieved

by calculating the mean of $\dot{U}_{highpass}$ over half a vibration period:

$$\dot{U}(t_k)_{bandpass} = \frac{\pi}{4f\Delta t} \sum_{n=k-\frac{1}{4f\Delta t}}^{k+\frac{1}{4f\Delta t}} \dot{U}(t_n)_{highpass}. \quad (5)$$

Ideally, eqn (5) suppresses higher harmonics of the order m by the factor $|[(-1)^m - 1]/2m|$, *i.e.*, even harmonics are zero while odd harmonics are damped proportional to $1/m$, $m = 1, 2, 3, \dots$. Thus, the major signal in $\dot{U}_{bandpass}$ represents the extrinsic tissue velocity of the first harmonic frequency, *i.e.*

$$\dot{U}(t_k)_{bandpass} \approx u_1(t_k) \cdot 2\pi f \cos(2\pi f t_k), \quad (6)$$

and therewith

$$U(t_k)_{bandpass} \approx \frac{1}{2\pi f} \dot{U}(t_k)_{bandpass}. \quad (7)$$

Equation (7) is valid for small time derivatives of u_1 , *i.e.* $\dot{u}_1 \ll \dot{U}$. $U_{bandpass}$ is finally transformed to the amplitude of the first harmonic extrinsic vibration $u : = u_1$ by

$$u(t_k) = \frac{\pi}{2f\Delta t} \sum_{n=k-\frac{1}{2f\Delta t}}^{k+\frac{1}{2f\Delta t}} |U(t_n)_{bandpass}|. \quad (8)$$

Displacements were estimated in eqn (2) by the phase-root-seeking algorithm (Pesavento *et al.* 1999; Eder *et al.* 2007), which required the computationally costly Fourier transform and, thus, most of the signal processing time. All subsequent filters were based on simple addition and subtraction operations of a maximum of $f\Delta t = 28$ samples. A diagram of signal processing is shown in Figure 3.

Offline signal processing

At the end of an experiment, the last 7.1 s of data were stored in memory for off-line signal processing implemented in Matlab (The MathWorks Inc., Natick, MA, USA). Off-line signal processing included averaging of wave amplitudes within the systolic and diastolic cardiac phase, yielding $u(systole)$ and $u(diastole)$ averaged over at least three R-R intervals. The cardiac phases were assigned to systole and diastole by a trained radiologist with respect to both the simultaneously acquired ECG and lateral wall motion. R-R intervals compromised by chest motion artifacts due to breathing or probe displacement were excluded from further analysis. We then tabulated isovolumetric cardiac time intervals using a WAV-based metric as introduced in (Elgeti *et al.* 2010b). The time delay between the decrease in u at early systole

and the cardiac motion u_{card} toward the ultrasound transducer was assigned to the cardiac phase of isovolumetric contraction (IVC). Correspondingly, the time delay between the increase in u at early diastole and the cardiac motion u_{card} away from the transducer was assigned to isovolumetric relaxation (IVR). The durations of IVC and IVR were deduced by means of the superposition of wave amplitudes $u(t)$ and cardiac motion $u_{card}(t)$. IVC was determined by manual selection of the time delay between the decaying branches of $u(t)$ and $u_{card}(t)$. Correspondingly, IVR was determined from the delay between the ascending branches of both functions. More specifically, the time instants t_1 and t_2 were selected from $u(t_1) = (u[diastole] + u[systole])/2$ and $u_{card}(t_2) = (u_{card}[diastole] + u_{card}[systole])/2$, which directly yield $IVC = t_2 - t_1$ at the descending branch of both graphs (in early systole) and $IVR = t_2 - t_1$ at the ascending branch (in early diastole). An illustration of t_1 and t_2 is given in (Elgeti *et al.* 2010b). Figure 3 illustrates IVC and IVR by means of ultrasound elastography.

RESULTS

The group averaged R-R interval was measured with 0.96 ± 0.15 s corresponding to a heart rate of 57.6 ± 9 beats per min. Figure 4 shows an example of 30-Hz wave amplitudes during the cardiac cycle with vibration (u) and without vibration (u_0). Three observations can be made: (1) $u > u_0$ throughout the cardiac cycle; (2) u is small during systole and increases in diastole as also shown for the u_x and u_z components in MRE (Sack *et al.* 2009) (cf. Fig. 1); and (3) u_0 displays amplitudes that correspond to the 30-Hz component of heart sounds. On average, the u_0 amplitudes were $35.5 \mu\text{m} \pm 13.3 \mu\text{m}$ in all volunteers. Figure 5 shows the amplitudes of heart sounds u_0 , systolic waves $u(systole)$ and diastolic waves $u(diastole)$ of all 20 volunteers. In all but one volunteer we found $u_0 < u(systole) < u(diastole)$. One volunteer had higher heart sound amplitudes than systolic wave amplitudes. Generally, the wave amplitudes during systole and diastole appeared to be correlated. To study this correlation, the vibration amplitudes of the actuator were varied multiple times in three volunteers. The results are shown in Figure 6. In all three subjects $u(systole)$ increased linearly with $u(diastole)$ with similar slopes from 0.51 to 0.59. The group-averaged ratio in all volunteers determined by single measurements was 0.60 ± 0.13 . IVC and IVR intervals show that cardiac motion lags behind the alteration of vibration amplitudes. Both IVC and IVR times were on the order of 100 ms. Group-averaged values and standard deviations are given in Table 1.

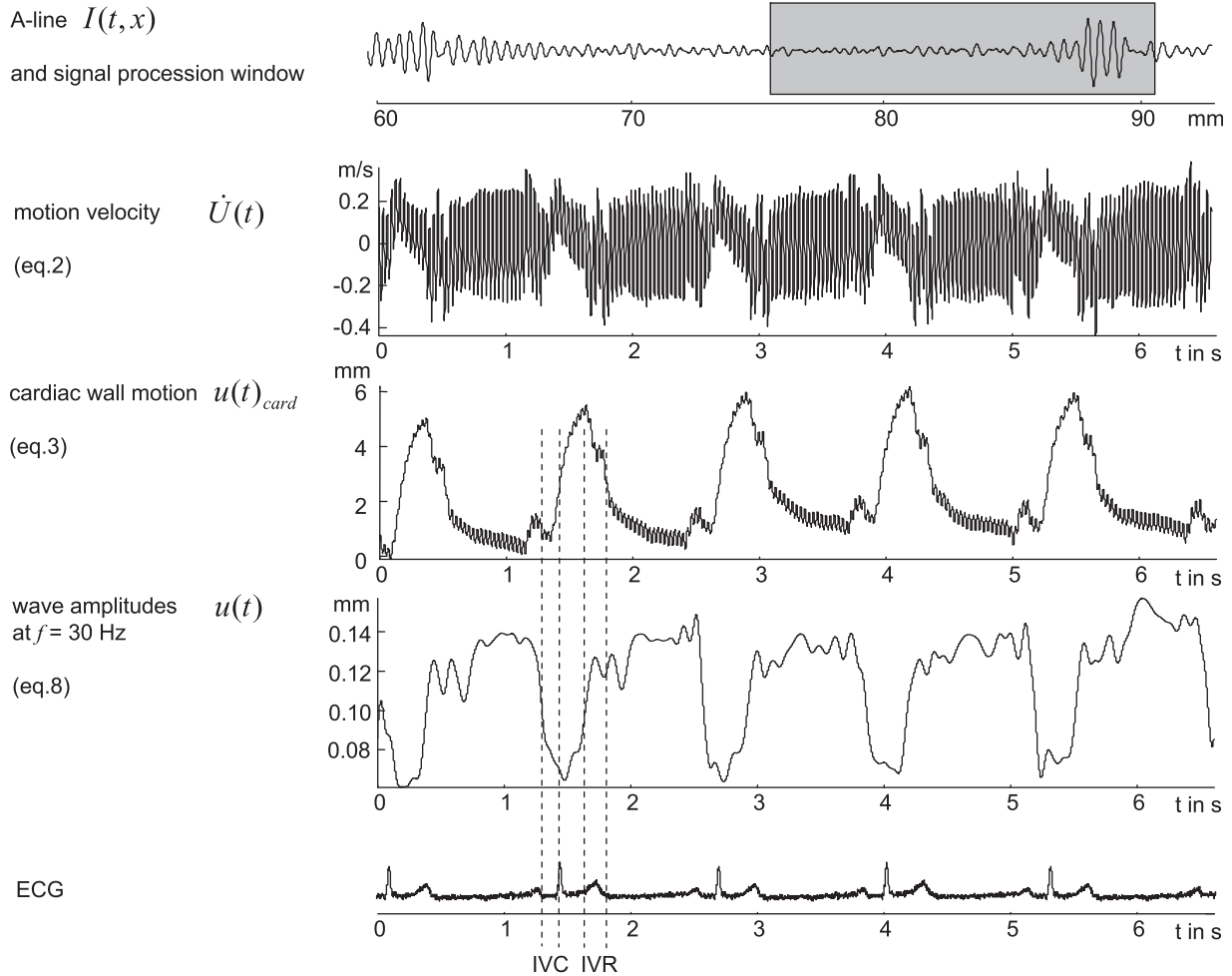


Fig. 3. Representation of real-time data output in our current setting consisting of (i) A-line with signal processing window (gray box); (ii) tissue velocity after cross-correlation-based displacement estimation mainly displays the externally induced 30-Hz vibration; (iii) cardiac wall motion after integrating $\dot{U}(t)$; (iv) wave amplitudes according to the real-time signal processing as described in the Methods section; and (v) electrocardiogram (ECG)-signal for the assignment of cardiac phases. Isovolumetric contraction (IVC) and isovolumetric relaxation (IVR) correspond to the isovolumetric phases during contraction and relaxation of the heart muscle, respectively.

DISCUSSION

Our study demonstrates the feasibility of time harmonic cardiac elastography in 20 healthy volunteers. Our method combines three major technical key points:

- (1) Real-time feedback on the scanning position and real-time estimation of wave amplitudes.
- (2) Actuator placement beneath the left lateral side of the chest and measurement of axial wave amplitude components in the lateral wall of the left ventricle along a parasternal line of sight.
- (3) Continuous harmonic stimulation of the chest by low-frequency vibration.

Point (1) is the prerequisite for choosing the optimal scanning position. After image guidance from standard

B-mode scans, the ultrasound transducer was positioned by an experienced cardiologist according to both the location of reflections along the A-line and the wave amplitude variation relative to the ECG. An apparent decrease in wave amplitudes during systole combined with the expected signal reflection at the cardiac wall indicated that the target tissue was within the processing window.

Point (2) defines the set-up of the actuator and the ultrasound scan line with respect to cardiac anatomy. Using A-line ultrasound combined with the proposed actuator, the chosen set-up assures most reproducible results consistent with findings in cardiac MRE.

Point (3) is necessary for sustaining a continuous flux of wave energy through the heart, which provides the elastodynamic foundation for the evaluation of wave amplitudes. Ideally, shear waves are planar and within an

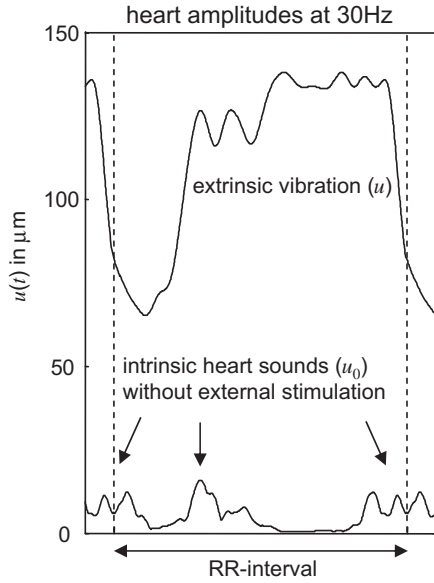


Fig. 4. Wave amplitudes at 30 Hz in the lateral wall of a healthy volunteer with and without external vibration, averaged over three cardiac cycles.

infinite isotropic, linear elastic and non-viscous medium of time-varying elasticity. Under this condition, a simple reciprocal relationship, $[u(\text{systole})/u(\text{diastole})]^4 = \mu(\text{diastole})/\mu(\text{systole})$, holds between shear wave amplitudes u and

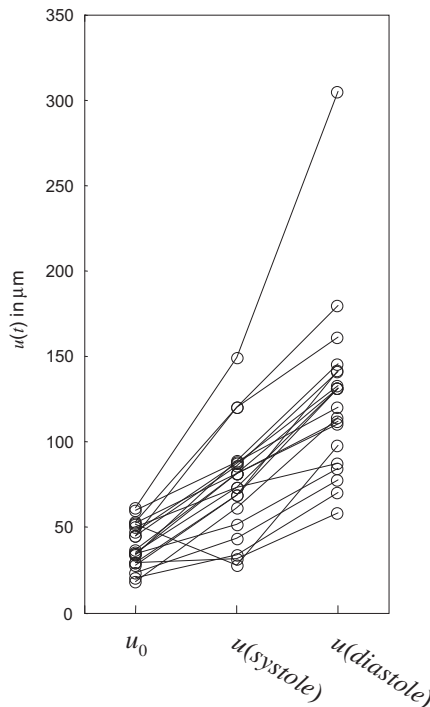


Fig. 5. Heart sound amplitudes at 30 Hz (u_0) and extrinsic vibration amplitudes during systole and diastole in the lateral wall of all 20 subjects investigated in this study.

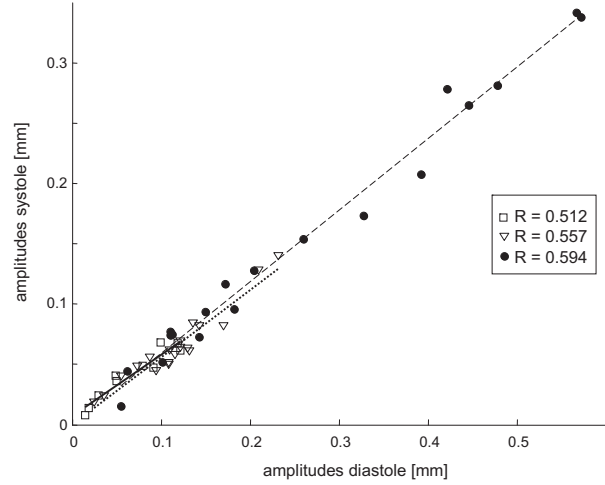


Fig. 6. Systolic wave amplitude versus diastolic wave amplitude in three volunteers at different vibration levels of the external mechanical actuator. Amplitude ratios R were measured by linear fits plotted by dashed, solid and dotted lines.

shear moduli μ (Sack *et al.* 2009). Shear waves inside the myocardium may be damped although viscous damping in muscle is known to be small at 30-Hz vibration frequency (Klatt *et al.* 2010). Attenuation may also arise from wave scattering, which clearly occurs in complex macroscopic structures such as the heart. Furthermore, finite media as the heart wall cause dispersion of the shear wave speed, which may also be affected by geometrical changes during the cardiac cycle. Finally, the heart is a highly non-isotropic wave propagation medium causing different shear wave velocities, depending on the polarization of the waves with respect to muscle fiber orientation. However, most of the aforementioned points are mitigated by a normalization of wave amplitudes at a time instant t_1 by the amplitudes at time t_2 . As a result, WAV-based elastography is limited to relative changes of myocardial elasticity. This strategy of normalization of wave amplitudes was demonstrated to provide consistent shear modulus ratios in cardiac MRE of animals (Elgeti *et al.* 2009), healthy volunteers (Elgeti *et al.* 2008) and patients (Elgeti *et al.* 2010a). It is a promising result of the present study that ultrasound can provide similar information as revealed by the far more elaborate MRI-based technique. This is intriguingly demonstrated by the wave amplitude ratio $u(\text{diastole})/u(\text{systole}) = 1.75 \pm 0.49$ and by the observation that intrinsic cardiac motion u_{card} lags approximately 100 ms behind the vibration-induced shear wave amplitude alteration u . Given the aforementioned reciprocal relationship between the shear wave amplitude and elasticity ratios, $\mu(\text{systole})/\mu(\text{diastole})$ is 14 ± 11 . In comparison, a group-averaged wave amplitude ratio of 1.58 ± 0.06 was reported in MRE of six volunteers by considering a large anatomical region along multiple short-axis slices through the left ventricle. On one hand, the higher standard deviation in our ultrasound-based study may be

Table 1. Group-averaged R-R interval from ECG and mean values derived from time-harmonic cardiac elastography

	R-R [s]	Min(u_0) [μm]	Max(u_0) [μm]	$u(\text{systole})$ [μm]	$u(\text{diastole})$ [μm]	$u(\text{systole})/u(\text{diastole})$	$U(\text{diastole})/U(\text{systole})$	u_{card} [mm]	IVC [ms]	IVR [ms]
Mean	0.96	2.8	39.5	76.0	126.7	0.60	1.75	4.6	99.3	104.0
SD	0.15	1.6	12.9	30.8	52.1	0.13	0.49	1.6	36.5	47.9

Mean and standard deviation (SD) correspond to the group response in 20 healthy volunteers. u_0 denotes the heart sound amplitudes at 30 Hz, i.e., $u(t)$ without external mechanical vibration. $u(\text{systole})$ and $u(\text{diastole})$ correspond to the amplitudes of 30-Hz vibrations during systole and diastole, respectively. u_{card} is the intrinsic myocardial motion. Isovolumetric contraction (IVC) and isovolumetric relaxation (IVR) are intervals derived by the WAV effect.

due to a larger group variability of physiologic parameter, e.g., given by BMI and heart rate. On the other hand, limitations of A-mode ultrasound as stated further down may have contributed to the variation of the WAV-effect in this study. The elasticity-based isovolumetric times measured by ultrasound show a similarly large variation as encountered in cardiac MRE (Elgeti et al. 2010b). The excellent time resolution achieved by the proposed ultrasound technique provides some insight into the cause underlying this variability: as seen in Figure 3 and Table 1, the presence of intrinsic heart sounds at 30 Hz causes a significant amount of wave amplitudes during isovolumetric intervals (Koiwa et al. 1991; Kanai 2009). This intrinsic vibration component certainly influences the descending and ascending branches of $u(t)$ during early systole and early diastole, respectively, thereby increasing the variability of our IVC and IVR times.

Limitations

Cardiac MRE provided *a priori* information about location and length of the measurement window for ultrasound-based cardiac elastography. Therefore, the method was not validated on animals. In general, A-mode ultrasound is limited by reduced spatial information and motion sensitivity constrained to axial displacements. Translation to the clinic would benefit from the simultaneous display of real-time motion tracking for time-harmonic elastography with standard B-mode echocardiography. At present, the target region is located in B-mode using an imaging probe, which is then replaced by the A-mode ultrasound transducer. This procedure is error prone and may produce positioning artifacts even if an experienced cardiologist acquires the ultrasonic echo data. Additionally, the window-based signal analysis is a limitation since regional relaxation abnormalities might not appear in mechanical parameters deduced from vibrations of the lateral wall.

In summary, we introduced a real-time ultrasound modality for analyzing externally stimulated continuous harmonic shear waves in the lateral heart wall. The shear wave amplitudes significantly changed during the cardiac cycle, giving rise to a distinct ratio of systolic to diastolic

wave amplitudes. Moreover, isovolumetric cardiac phases were estimated from the time difference of this amplitude change and the initiation of wall motion. The parameters related to externally induced shear vibrations of the heart reveal the alteration of myocardial relaxation and tension during the cardiac cycle and may provide a potentially important diagnostic marker for identifying myocardial relaxation abnormalities.

Acknowledgments—The authors gratefully acknowledge the financial support from the German Research Foundation DFG Sa 901/3 and Sa 901/8.

REFERENCES

- Aurigemma GP, Zile MR, Gaasch WH. Contractile behavior of the left ventricle in diastolic heart failure: With emphasis on regional systolic function. *Circulation* 2006;113:296–304.
- Bieri O, Maderwald S, Ladd ME, Scheffler K. Balanced alternating steady-state elastography. *Magn Reson Med* 2006;55:233–241.
- Bouchard RR, Hsu SJ, Wolf PD, Trahey GE. *In vivo* cardiac, acoustic-radiation-force-driven, shear wave velocimetry. *Ultrason Imaging* 2009;31:201–213.
- Dumont DM, Doherty JR, Trahey GE. Noninvasive assessment of wall-shear rate and vascular elasticity using combined ARFI/SWEI/spectral Doppler imaging system. *Ultrason Imaging* 2011;33:165–188.
- Eder A, Arnold T, Kargel C. Performance evaluation of displacement estimators for real-time ultrasonic strain and blood flow imaging with improved spatial resolution. *IEEE Trans Instrum Meas* 2007;56:1275–1284.
- Elgeti T, Beling M, Hamm B, Braun J, Sack I. Cardiac magnetic resonance elastography: Toward the diagnosis of abnormal myocardial relaxation. *Invest Radiol* 2010a;45:782–787.
- Elgeti T, Beling M, Hamm B, Braun J, Sack I. Elasticity-based determination of isovolumetric phases in the human heart. *J Cardiovasc Magn Reson* 2010b;12:60.
- Elgeti T, Laule M, Kaufels N, Schnorr J, Hamm B, Samani A, Braun J, Sack I. Cardiac MR elastography: Comparison with left ventricular pressure measurement. *J Cardiovasc Magn Reson* 2009;11:44.
- Elgeti T, Rump J, Papazoglou S, Hamhaber U, Hamm B, Braun J, Sack I. Cardiac magnetic resonance elastography—Initial results. *Invest Radiol* 2008;43:762–772.
- Hsu SJ, Bouchard RR, Dumont DM, Wolf PD, Trahey GE. *In vivo* assessment of myocardial stiffness with acoustic radiation force impulse imaging. *Ultrasound Med Biol* 2007;33:1706–1719.
- Kanai H. Propagation of spontaneously actuated pulsive vibration in human heart wall and *in vivo* viscoelasticity estimation. *IEEE Trans Ultrason Ferroelectr Freq Control* 2005;52:1931–1942.
- Kanai H. Propagation of vibration caused by electrical excitation in the normal human heart. *Ultrasound Med Biol* 2009;35:936–948.
- Klatt D, Papazoglou S, Braun J, Sack I. Viscoelasticity-based magnetic resonance elastography of skeletal muscle. *Phys Med Biol* 2010;55:6445–6459.
- Koiwa Y, Ohyama T, Takagi T, Kikuchi J, Honda H, Shimizu Y, Hashiguchi R, Shirato K, Takishima T. Vibration analysis of the

- human left ventricular posterobasal wall at the moment of the first heart sound emission. *Tohoku J Exp Med* 1991;164:125–144.
- Kolipaka A, Araoz PA, McGee KP, Manduca A, Ehman RL. Magnetic resonance elastography as a method for the assessment of effective myocardial stiffness throughout the cardiac cycle. *Magn Reson Med* 2010;64:862–870.
- Konofagou EE, D'Hooge J, Ophir J. Myocardial elastography—A feasibility study *in vivo*. *Ultrasound Med Biol* 2002;28:475–482.
- Lee WN, Provost J, Fujikura K, Wang J, Konofagou EE. *In vivo* study of myocardial elastography under graded ischemia conditions. *Phys Med Biol* 2011;56:1155–1172.
- Maurice RL, Fromageau J, Cardinal MH, Doyley M, de Muinck E, Robb J, Cloutier G. Characterization of atherosclerotic plaques and mural thrombi with intravascular ultrasound elastography: A potential method evaluated in an aortic rabbit model and a human coronary artery. *IEEE Trans Inf Technol Biomed* 2008;12:290–298.
- Muthupillai R, Ehman RL. Magnetic resonance elastography. *Nat Med* 1996;2:601–603.
- Nenadic IZ, Urban MW, Mitchell SA, Greenleaf JF. Lamb wave dispersion ultrasound vibrometry (LDUV) method for quantifying mechanical properties of viscoelastic solids. *Phys Med Biol* 2011;56:2245–2264.
- Ophir J, Cespedes I, Ponnekanti H, Yazdi Y, Li X. Elastography: A quantitative method for imaging the elasticity of biological tissues. *Ultrason Imaging* 1991;13:111–13134.
- Parker KJ, Huang SR, Musulin RA, Lerner RM. Tissue response to mechanical vibrations for “sonoelasticity imaging”. *Ultrasound Med Biol* 1990;16:241–246.
- Pesavento A, Perrey C, Krueger M, Ermert A. A time-efficient and accurate strain estimation concept for ultrasonic elastography using iterative phase zero estimation. *IEEE Trans Ultrason Ferroelectr Freq Control* 1999;46:1057–1067.
- Pislaru C, Urban MW, Nenadic I, Greenleaf JF. Shearwave dispersion ultrasound vibrometry applied to *in vivo* myocardium. *Conf Proc IEEE Eng Med Biol Soc* 2009;2891–2894.
- Plewes DB, Betty I, Urchuk SN, Soutar I. Visualizing tissue compliance with MR imaging. *J Magn Reson Imaging* 1995;5:733–738.
- Robert B, Sinkus R, Gennisson JL, Fink M. Application of DENSE-MR-elastography to the human heart. *Magn Reson Med* 2009;62:1155–1163.
- Rump J, Klatt D, Braun J, Warmuth C, Sack I. Fractional encoding of harmonic motions in MR elastography. *Magn Reson Med* 2007;57:388–395.
- Sack I, Rump J, Elgeti T, Samani A, Braun J. MR elastography of the human heart: Noninvasive assessment of myocardial elasticity changes by shear wave amplitude variations. *Magn Reson Med* 2009;61:668–677.
- Schaar JA, de Korte CL, Mastik F, van Damme LC, Krams R, Serruys PW, van der Steen AF. Three-dimensional palpography of human coronary arteries. *Ex vivo* validation and in-patient evaluation. *Herz* 2005;30:125–133.
- Vappou J, Luo J, Konofagou EE. Pulse wave imaging for noninvasive and quantitative measurement of arterial stiffness *in vivo*. *Am J Hypertens* 2010;23:393–398.
- Varghese T, Zagzebski JA, Rahko P, Breburda CS. Ultrasonic imaging of myocardial strain using cardiac elastography. *Ultrason Imaging* 2003;25:1–16.
- Wells PN, Liang HD. Medical ultrasound: Imaging of soft tissue strain and elasticity. *J Royal Soc Interface* 2011;8:1521–1549.
- Zile MR, Baicu CF, Gaasch WH. Diastolic heart failure—Abnormalities in active relaxation and passive stiffness of the left ventricle. *N Engl J Med* 2004;350:1953–1959.